

DOI: 10.1002/cssc.201100211

Nanostructured Membranes for Enzyme Catalysis and Green Synthesis of Nanoparticles

Vasile Smuleac,^[a] Rajender Varma,^[b] Babita Baruwati,^[b] Subhas Sikdar,^[b] and Dibakar Bhattacharyya^{*[a]}

Macroporous membranes functionalized with ionizable macromolecules provide promising applications in high capacity toxic metal capture, nanoparticle syntheses, and catalysis. Our low-pressure membrane approach has good reaction and separation selectivities, which are tunable by varying pH, ionic strength, or pressure. The sustainable green chemistry approach under ambient conditions and the evaluation of a reactive poly(acrylic acid) (PAA)-modified polyvinylidene fluoride (PVDF) membrane is described. Two distinct membrane types

were obtained through different methods: 1) a stacked membrane through layer-by-layer assembly for the incorporation of enzymes (catalase and glucose oxidase), providing tunable product yields and 2) Fe/Pd nanoparticles for degradation of pollutants, obtained through an in situ green synthesis. Bioreactor–nanodomain interactions and mixed matrix nanocomposite membranes provide remarkable versatility compared to conventional membranes.

Membrane-based separations and reactions have wide applications ranging from clean water production to selective separations, chemical synthesis, and biotechnology.^[1–3] The availability of high-capacity membranes for efficient, selective catalysis with facile in situ regeneration is much needed for economic and sustainable exploitation of a variety of applications, such as green synthesis of chemicals, toxic metals removal, or toxic organics destruction in polluted water. Despite tremendous advances in separation science, membranes with superior selectivity are still desirable. An example of remarkable selectivity found in nature is in biological membranes containing aquaporins, which transport water at high rates with complete removal of protons.^[4,5] The advances in self-assembled^[6,7] carbon^[8] nanotubes and alumina nanochannels^[9,10] and nanocomposite membranes^[11,12] have provided elegant techniques with high permeability and selectivity.

Functionalization of microfiltration-type membranes with polymers and biomolecules^[13,14] to create nanostructured domains in pores offers high transmembrane flux and exceptional versatility, extending their application from separations to toxic metal capture, nanoparticle synthesis, and catalytic reactions. If the selected macromolecule is a polyelectrolyte, the incorporation in the membrane pores provides both highly charged field and high toxic metal sorption capacity (Figure 1 a).^[15] The metal-sorbed membrane can be easily converted to catalytic membranes (Figure 1 b) through reduction to metallic nanoparticles. The electrostatic assembly based on layer-by-layer (LbL) deposition of polyelectrolytes can be used for the incorporation of active enzymes (Figure 1 c) without covalent attachment.

Reactive, catalytic membranes have been studied and a common platform, poly(acrylic acid) (PAA)-functionalized polyvinylidene fluoride (PVDF) membrane (650 nm pore size), was used as a support for 1) enzyme incorporation using the LbL technique for the formation of multilayer membrane bioreac-

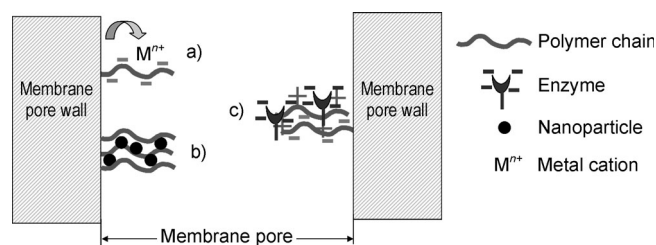


Figure 1. Multifunctional membranes for metal capture and catalytic reactions. a) Single charged polymer layer for toxic metal capture; b) Supported metallic NPs for catalysis; c) Electrostatic enzyme immobilization in LbL assembly for catalysis.

tors and 2) in situ synthesis of metal nanoparticles using a “green” reducing agent (vitamin C) for environmentally important reactions. All functionalization steps, including enzyme incorporation and nanoparticle formation, were carried out using water-based chemistry.

Results and Discussion

The LbL technique is simple and versatile; it most commonly involves the alternate deposition of oppositely charged polymer layers and is suitable for the assembly of complex supra-

[a] Dr. V. Smuleac, Prof. D. Bhattacharyya
Dept. of Chemical and Materials Engineering
University of Kentucky
Lexington, KY 40506 (USA)
Fax: (+1) 859 323 1929
E-mail: db@engr.uky.edu

[b] Dr. R. Varma, Dr. B. Baruwati, Dr. S. Sikdar
Sustainable Technology Division
National Risk Management Research Lab/USEPA
Cincinnati, OH 45268 (USA)

Supporting Information for this article is available on the WWW under <http://dx.doi.org/10.1002/cssc.201100211>.

molecular structures^[16,17] and the incorporation of enzymes without covalent attachment. Other techniques, such as site-directed immobilization,^[18] usually employ complex and expensive molecular biology methodologies. We aim to use a simple method for enzyme immobilization that ensures high catalytic activity and stability as well as the versatility required for the electrostatic immobilization of various enzymes.

Stacked membranes for enzymatic catalysis

The chemical or pharmaceutical industries often use several reactions (e.g., parallel, sequential, etc.) for syntheses; many separation and purification steps are needed to obtain a pure product with high yield, which increases energy consumption and cost. Bifunctional catalytic membranes can, however, be synthesized easily and applied to reactions to obtain high selectivity and product yield with minimal separation steps. This is illustrated in Figure 2, in which two model enzymes are

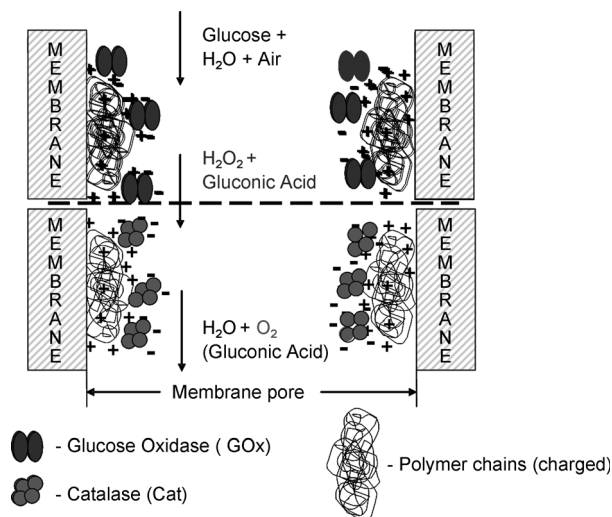
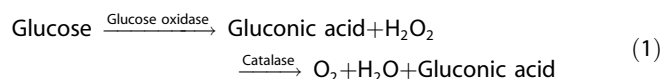


Figure 2. Bifunctional enzyme-catalyzed reactions in nanostructured membranes.

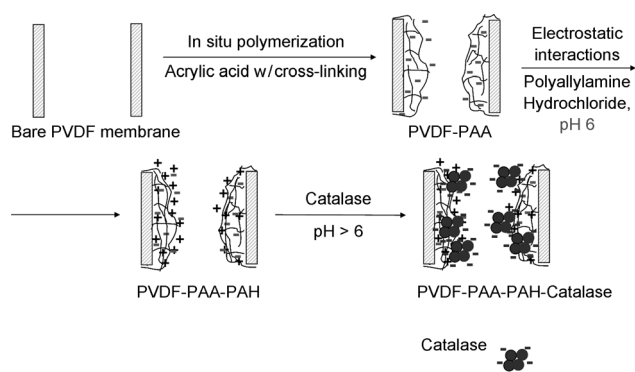
used, that is glucose oxidase immobilized on the upper membrane and catalase on the lower. In this particular system, the hydrogen peroxide reaction product in the first membrane is the reactant in the second, as detailed in Equation (1). Gluconic acid, a high value chemical commonly used in calcium or iron(II) gluconate nutrition supplements, is obtained without additional separation steps.



Glucose oxidase, immobilized through LbL assembly on various membranes, have been reported previously.^[19,20] We use an immobilized catalase enzyme in a polyelectrolyte multilayer assembly formed within the membrane pore domain under convective conditions. The PVDF membrane was functionalized with PAA by in situ polymerization of acrylic acid, as described

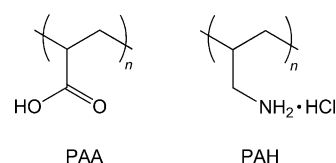
in the Experimental Section; subsequent deposition occurred through multiple electrostatic interactions between the adsorbing polyelectrolyte and the oppositely charged layer already on the membrane. Poly(allylamine) hydrochloride (PAH) comprised the a second layer to form a PAA–PAH-functionalized PVDF membrane with an overall positive charge.

Enzyme immobilization on the polyelectrolyte-assembled membranes occurs through electrostatic interactions. Catalase (isoelectric point, $pI=5.7$) was immobilized on positively charged membranes at pH 7 to give catalase an overall negative charge for easy incorporation into a positively charged membrane [PAA–PAH, $pK_a(\text{PAH})\approx 8.8$]. The membrane coating, assembly formation, and catalase incorporation sequence is shown in Scheme 1. The second enzyme, glucose oxidase ($pI=$



Scheme 1. PVDF membrane modification inside pores with charged polymers and catalase immobilization.

4.2) was immobilized in a three-layer assembly consisting of PAA–PAH–PSS, which carries an overall negative charge (PSS = polystyrene sulfonate). This was conducted at pH 7, at which



glucose oxidase has an overall positive charge, opposite to that of the membrane. This enzyme catalyzes the well-known reaction $2\text{H}_2\text{O}_2 \rightarrow 2\text{H}_2\text{O} + \text{O}_2$.

Catalase activities in the free and immobilized forms were evaluated by using the Michaelis–Menten model, the rate data for which was obtained under a pressure-driven convective flow, ensuring accessibility to all active sites. Figure 3a shows the hydrogen peroxide degradation rates at four substrate concentrations. At saturation conditions the membrane-immobilized catalase activity is very similar to that of homogeneous phase catalysis (90%), which is superior to many immobilization techniques. It is well known that other common enzyme immobilization techniques,^[18] such as covalent attachment, result in significant loss of activity. In particular, glucose oxidase has demonstrated a sevenfold reduction in activity upon

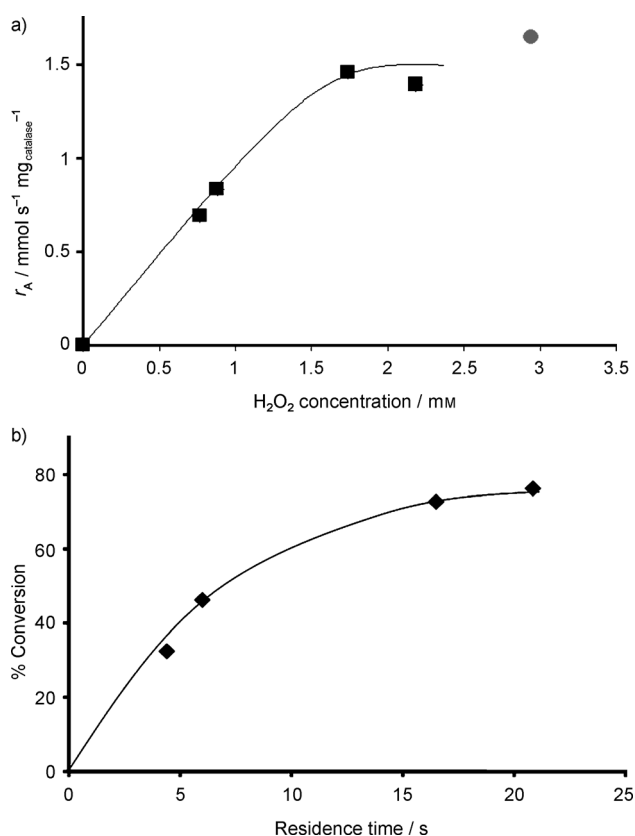
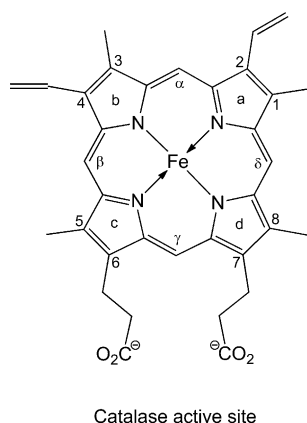


Figure 3. a) Rate of hydrogen peroxide decomposition as a function of substrate concentration at pH 6.92, $t = 22^\circ\text{C}$, $[\text{H}_2\text{O}_2]_{\text{initial}} = 2.9 \text{ mM}$, using 0.17 mg of immobilized catalase (■) or 0.31 mg of catalase homogeneous phase (●); b) Hydrogen peroxide conversion as a function of residence time in the membrane pore with catalase enzyme in an LbL assembly at pH 6.92, $t = 22^\circ\text{C}$, $[\text{H}_2\text{O}_2]_{\text{initial}} = 2.9 \text{ mM}$, using 0.17 mg of immobilized catalase, and showing the immobilized catalase activity to be 90% that of homogenous phase catalysis ($\text{mmol}_{\text{H}_2\text{O}_2} \text{min}^{-1} \text{mg}_{\text{enzyme}}^{-1}$).

covalent immobilization on a porous alumina support compared with the activity in the homogeneous (bulk) phase.^[21]

Further to reports on catalase immobilization on various supports,^[22] our approach allows for the tuning of product yield through variation of residence time (τ) in membrane pores. The residence time was calculated as $\tau = V/(AJ_v)$, where V is the membrane volume, A the external area (33.2 cm^2), and

J_v the permeation flux ($\text{cm}^3 \text{ cm}^2 \text{ s}^{-1}$) through volume V . In addition, $V = \varepsilon AL$, where ε is the porosity (70% average, from manufacturer's data) and L the membrane thickness ($125 \mu\text{m}$). The flux (and hence τ) can be modulated by changing the applied pressure; varying the pressure between 30 and 140 kPa caused a flux change from $3\text{--}12 \times 10^{-4} \text{ cm}^3 \text{ cm}^2 \text{ s}^{-1}$. Low pressure operations reduce energy consumption significantly. The relationship between the residence time and reactant conversion at steady state is shown in Figure 3 b. Variation of operating pressure can therefore modulate product yield as well as flux (i.e., throughput rates).

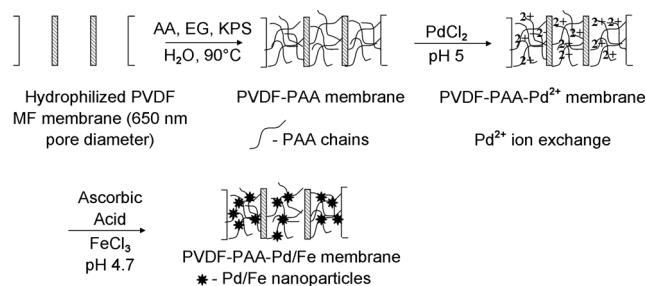
In addition to the development of individual membranes, the in situ hydrogen peroxide generation was investigated using the membrane reactors in series described above (Figure 2). The upper membrane contained glucose oxidase and the lower catalase, which were incorporated at pH 7 into a PAA-PAH-PSS and PAA-PAH layer assembly, respectively. To prove the in situ hydrogen peroxide formation, the upper membrane was mounted in a filtration cell and an aerated pH 7 feed solution containing 0.2 L of 50 mM glucose was passed convectively through the membrane. After a residence time of 0.7 s (flux of $12.6 \times 10^{-4} \text{ cm}^3 \text{ cm}^2 \text{ s}$ at a pressure of 140 kPa), permeate solutions were found to contain 0.9 mM of H_2O_2 . Two membranes containing glucose oxidase and catalase, respectively, were then mounted in the filtration cell using the aforementioned procedure. The concentration of hydrogen peroxide in the permeate was found to be zero (i.e., 100% conversion of H_2O_2 to oxygen by catalase). Even with an eightfold (ca. 5.3 s) increase in residence time, the H_2O_2 conversion was still 100%. This is owed to the excess of catalase (21300 vs 1550 units of glucose oxidase; for glucose oxidase, one unit oxidizes 1.0 μmol of β -D-glucose to D-gluconolactone and H_2O_2 per min at pH 5.1 and 35°C ; whereas for catalase, one unit decomposes 1.0 μmol of H_2O_2 per min at pH 7.0 and 25°C) in the LbL assembly, however, these loadings are easily adjustable for specific conversion requirements.

Green synthesis of bimetallic nanoparticles in membranes

The same PAA-functionalized (for metal ion capture) membrane platform was extended to synthesize metal nanoparticles (NPs) in membrane pores using a greener method. The properties of nanoscale metal particles often differ from those of bulk materials, enabling applications in areas such as heterogeneous catalysis,^[23] magnetism,^[24] or molecular biology.^[25] For water purification applications, particularly those involving detoxification of chlorinated organics, the Fe and Fe/Pd bimetallic NP systems are commonly used,^[26] although other systems such as Fe/Ni and Fe/Cu have also been reported.^[27,28] Owing to their magnetic properties, Fe (or Fe/Pd bimetallic), NPs tend to agglomerate rapidly in water to form micron-size or larger aggregates, thus losing reactivity.^[29] Various techniques have been employed to control the particle size by using additives or coating with a protective layer.^[26,29] Another approach to control the particle size and prevent agglomeration is to synthesize supported particles; we have used the PAA-coated PVDF membrane extensively as a platform for this purpose.

In contrast to other work that has reported the use of toxic borohydride as a reducing agent,^[30] we show that highly reactive NPs (Fe, Pd, or Fe/Pd) can be synthesized easily in membranes using “green” reducing agents. Nontoxic, biodegradable materials, such as ascorbic acid (vitamin C),^[31–33] grape pomace,^[34] or polymers,^[35] have been recently applied to homogeneous phase Fe/Pd NP synthesis. We report the synthesis of supported Fe/Pd NPs in membrane pores using ascorbic acid as a reducing agent.

A “green” synthesis of bimetallic Fe/Pd NPs in PAA-functionalized PVDF membranes is shown in Scheme 2. The first step, PAA coating on PVDF membrane, is described in the Experi-



Scheme 2. PVDF membrane modification inside pores with charged polymers and subsequent Fe/Pd NP synthesis, where AA is acrylic acid, EG is ethylene glycol (cross-linking agent), and KPS is potassium persulfate (initiator).

mental Section. Prior to ion exchange, PAA-functionalized PVDF membranes were immersed in a NaCl (5–10 wt.%) solution at pH 10 for at least 3 h to convert –COOH to the –COONa form. In the next step, the membrane was washed with deionized ultrafiltered water until the pH of the washing solution became neutral. The membrane was then immersed in PdCl₂ solution at pH 4.7 for 3 h. Feed solution volume and concentration were typically 50 mL and 20 mg_{Pd²⁺} L⁻¹, respectively. Nitrogen gas was bubbled through the feed solution to minimize oxidation. Reduction with ascorbic acid (50 mL, 0.1 M) in the presence of FeCl₃ (180 mg_{Fe} L⁻¹) ensured Fe/Pd bimetallic NP formation.

Bimetallic Fe/Pd particles were also formed in diffusion mode; the experimental setup is shown in the Supporting Information, Figure S1. The PVDF–PAA membrane was mounted between two chambers, one containing K₂PdCl₄ and the other a mixture of FeCl₃ and ascorbic acid; each diffused inside the membrane pores. As a consequence, the Fe/Pd NPs were formed primarily in the membrane pores rather than on the surface layer; this is the major difference between the diffusive and soaking modes. In the latter approach the NPs are formed both on the surface layer and within the membrane pores.

The reduction potential ($E^0 = 0.06$ V) of ascorbic acid is sufficient to reduce Pd²⁺ ($E^0 = 0.951$ V), but not Fe²⁺ ($E^0 = -0.44$ V). Ascorbic acid can, however, simultaneously reduce the Fe and Pd, as shown in Figure 4 a. The overall potential for the three reactions is positive (negative free energy), enabling the reduction of Pd²⁺ and Fe²⁺ to Pd⁰ and Fe⁰, respectively. An SEM image of the Fe/Pd NPs after using ascorbic acid as reducing

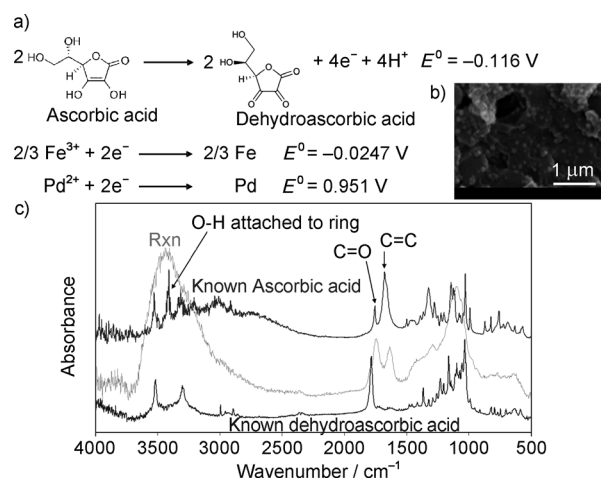


Figure 4. a) Fe and Pd reduction with ascorbic acid; b) SEM of the Fe/Pd NP immobilized on the membrane; and c) FTIR spectrum before (ascorbic acid) and after (dehydroxyascorbic acid) reduction.

agent is shown in Figure 4b. The NPs are uniform, with an average size of approximately 30 nm. The bimetallic NP composition was 3.1 wt.% Pd relative to Fe; an energy dispersive X-ray spectrum and elemental analysis is shown in the Supporting Information, Figure S2.

The presence of Fe [(110), (200)] and Pd [(111), (200)] peaks in the NP EDX pattern showed iron to be in metallic α -Fe form. In the simultaneous reduction of Fe and Pd, ascorbic acid is oxidized to dehydroascorbic acid. The FTIR spectrum in Figure 4c, “Rxn” line, shows a new peak in the 1750–1680 cm⁻¹ region, corresponding to the C=O stretching frequency of the ketone bond formed in the reaction.

Conclusions

We have developed a simple and versatile method of enzyme catalysis and nanoparticle synthesis using a common platform, poly(acrylic acid)-coated polyvinylidene fluoride membrane, and “greener” methods. The enzymes were incorporated in polymer multilayer-assembled membranes through electrostatic interactions and maintained a high activity upon immobilization comparable to that of the homogeneous phase catalysis. Membranes containing different enzymes can be stacked and used as reactors in series and the reaction yields can be modulated by adjusting parameters such as the enzyme loading on each membrane and the residence time, which is in turn related to permeate flux. We have demonstrated the direct and “green” synthesis of bimetallic Fe/Pd particles in a membrane domain. Compared to the established method, which uses toxic sodium borohydride, this approach uses biodegradable ascorbic acid and thus has a minimized environmental impact.

Experimental Section

PVDF membranes with a thickness of 125 μm and an average pore size of 650 nm were purchased from Millipore. Glucose oxidase from *Aspergillus niger* and catalase from bovine liver were pur-

chased from Aldrich; acrylic acid, ascorbic acid, dehydroascorbic acid, palladium chloride, potassium tetrachloropalladate(II), titanium(IV) oxysulfate, and PAH and PSS (average MW \approx 70 000 g mol⁻¹) were supplied by Aldrich. The protein assay kit was obtained from BioRad Laboratories. Trichloroethylene, ferric chloride hexahydrate, hydrogen peroxide, sodium hydroxide, and deionized ultrafiltered water were purchased from Fisher Scientific. Ethylene glycol and potassium persulfate were purchased from Mallinckrodt and EM Science, respectively.

PVDF membranes were functionalized with poly(acrylic acid) through in situ polymerization of acrylic acid. The polymerization reaction was carried out in aqueous solution, comprising 30% acrylic acid, the cross-linking agent ethylene glycol (molar ratio ethylene glycol/acrylic acid = 1:6.5) and the initiator potassium persulfate (1 wt.%). The PVDF membrane^[36] was dipped in the polymerization solution for 2 min, sandwiched between two Teflon plates and placed in an oven at 90 °C for 4 h. Nitrogen gas was supplied continuously to flush out oxygen, which acts as an inhibitor for the polymerization reaction. To ensure thorough wetting, hydrophilic PVDF membranes were used.

The amount of enzyme in the feed and permeate solutions was determined using the Bradford protein assay procedure.^[37] A calibration curve was obtained from a bovine serum albumin standard solution. An acidic dye was then added to the protein solution, and the absorbance of the dye-protein complex was measured at 595 nm, with a standard deviation for three measurements of less than 0.1%. The amount of enzyme immobilized on the membrane could be estimated by material balance analysis.

Hydrogen peroxide degradation was analyzed by using a well established colorimetric method.^[38] An acidified titanium(IV) oxysulfate solution was added, and the absorbance of the yellow-colored titanium-peroxo complex was measured at 407 nm. Over the concentration range 2–100 mg L⁻¹, the standard deviation was less than 0.5%.

The amount of Pd captured during ion exchange and Fe reduced in the presence of ascorbic acid was determined by material balance analysis. The concentrations for Fe and Pd in the feed and permeate solutions were quantified by using a Varian SpectraAA 220 fast sequential atomic absorption spectrometer equipped with a Fisher Scientific hollow cathode lamp. For measurements involving Fe, the lamp was operated at a wavelength of 386.0 nm and the calibration plot created by using four different concentrations of Fe ranging from 25 to 200 mg L⁻¹; $R^2 = 0.9993$ and the average analytical error was 2%. For Pd measurements, the lamp was operated at a wavelength of 246.6 nm and the linear calibration range was between 0.2 and 28 mg L⁻¹ Pd, with an analysis error of less than 2%.

Acknowledgements

This study was supported by the NIEHS-SRP program and by DOE-KRCEE.

Keywords: electrostatic interactions · enzymes · immobilization · membranes · nanoparticles

[1] E. Drioli, L. Giorno, *Comprehensive Membrane Science and Engineering*, Elsevier, Amsterdam, 2010.

- [2] M. A. Shannon, P. W. Bohn, M. Elimelech, J. G. Georgiadis, B. J. Marinas, A. M. Mayes, *Nature* **2008**, *452*, 301–310.
- [3] N. N. Li, A. G. Fane, W. S. W. Ho, T. Matsuura, *Advanced Membrane Technology and Applications*, Wiley & Sons, New York, **2008**.
- [4] D. Fu, A. Libson, L. J. W. Miercke, C. Weltzman, P. Nollert, J. Krucinski, R. M. Stroud, *Science* **2000**, *290*, 481–486.
- [5] E. Tajkhorshid, P. Nollert, M. O. Jensen, L. J. W. Miercke, J. O'Connell, R. M. Stroud, K. Schulten, *Science* **2002**, *296*, 525–530.
- [6] E. N. Savariar, K. Krishnamoorthy, S. Thayumanavan, *Nat. Nanotechnol.* **2008**, *3*, 112–117.
- [7] P. Kohli, C. C. Harrell, Z. Cao, R. Gasparac, W. Tan, C. R. Martin, *Science* **2004**, *305*, 984–986.
- [8] B. J. Hinds, N. Chopra, T. Rantell, R. Andrews, V. Gavalas, L. G. Bachas, *Science* **2004**, *303*, 62–65.
- [9] T. C. Merkel, B. D. Freeman, R. J. Spontak, Z. He, I. Pinnau, P. Meakin, A. J. Hill, *Science* **2002**, *296*, 519–522.
- [10] W. Yave, K. V. Peinemann, S. Shishatskiy, V. Khotimskiy, M. Chirkova, S. Matson, E. Litvinova, N. Lecerf, *Macromolecules* **2007**, *40*, 8991–8998.
- [11] W. Chen, Z. Q. Wu, X. H. Xia, J. J. Xu, H. Y. Chen, *Angew. Chem.* **2010**, *122*, 8115–8119; *Angew. Chem. Int. Ed.* **2010**, *49*, 7943–7947.
- [12] S. J. Li, J. Li, K. Wang, C. Wang, J. J. Xu, H. Y. Chen, X. H. Xia, Q. Huo, *ACS Nano* **2010**, *4*, 6417–6424.
- [13] M. Ulbricht, *Polymer* **2006**, *47*, 2217–2262.
- [14] M. L. Bruening, D. M. Dotzauer, P. Jain, L. Ouyang, G. L. Baker, *Langmuir* **2008**, *24*, 7663–7673.
- [15] S. M. C. Ritchie, L. G. Bachas, T. Olin, S. K. Sikdar, D. Bhattacharyya, *Langmuir* **1999**, *15*, 6346–6357.
- [16] G. Decher, *Science* **1997**, *277*, 1232–1237.
- [17] O. Ikkala, G. Brinke, *Science* **2002**, *295*, 2407–2409.
- [18] D. A. Butterfield, D. Bhattacharyya, S. Daunert, L. G. Bachas, *J. Membr. Sci.* **2001**, *181*, 29–37.
- [19] V. Smuleac, D. A. Butterfield, D. Bhattacharyya, *Langmuir* **2006**, *22*, 10118–10124.
- [20] S. Datta, C. Cecil, D. Bhattacharyya, *Ind. Eng. Chem. Res.* **2008**, *47*, 4586–4597.
- [21] S. J. Li, C. Wang, Z. Q. Wu, J. J. Xu, X. H. Xia, H. Y. Chen, *Chem. Eur. J.* **2010**, *16*, 10186–10194.
- [22] Y. Wang, F. Caruso, *Adv. Funct. Mater.* **2004**, *14*, 1012–1018.
- [23] F. Tao, M. E. Grass, Y. Zhang, D. R. Butcher, J. R. Renzas, Z. Li, J. Y. Chung, B. S. Mun, M. Salmeron, G. A. Somorjai, *Science* **2008**, *322*, 932–934.
- [24] S. Sun, C. B. Murray, D. Weller, L. Folks, A. Moser, *Science* **2000**, *287*, 1989–1992.
- [25] N. L. Rosi, D. A. Giljohann, C. S. Thaxton, A. K. R. Lytton-Jean, M. S. Han, C. A. Mirkin, *Science* **2006**, *312*, 1027–1129.
- [26] F. He, D. Zhao, *Appl. Catal. B* **2008**, *84*, 533–540.
- [27] B. Schrick, J. L. Blough, A. D. Jones, T. E. Mallouk, *Chem. Mater.* **2002**, *14*, 5140–5147.
- [28] N. Zhu, H. Luan, S. Yuan, J. Chen, X. Wu, L. Wang, *J. Hazard. Mater.* **2010**, *176*, 1101–1105.
- [29] A. H. Lu, E. L. Salabas, F. Schuth, *Angew. Chem.* **2007**, *119*, 1242–1266; *Angew. Chem. Int. Ed.* **2007**, *46*, 1222–1244.
- [30] J. Xu, D. Bhattacharyya, *J. Phys. Chem. C* **2008**, *112*, 9133–9144.
- [31] M. N. Nadagouda, R. S. Varma, *Cryst. Growth Des.* **2007**, *7*, 2582–2587.
- [32] F. He, J. Liu, C. B. Roberts, D. Zhao, *Ind. Eng. Chem. Res.* **2009**, *48*, 6550–6557.
- [33] J. Liu, F. He, T. M. Gunn, D. Zhao, C. B. Roberts, *Langmuir* **2009**, *25*, 7116–7128.
- [34] B. Baruwati, R. S. Varma, *ChemSusChem* **2009**, *2*, 1041–1044.
- [35] J. Virkutyte, R. S. Varma, *Chem. Sci.* **2011**, *2*, 837–846.
- [36] V. Smuleac, L. G. Bachas, D. Bhattacharyya, *J. Membr. Sci.* **2010**, *346*, 310–317.
- [37] M. M. Bradford, *Anal. Biochem.* **1976**, *72*, 248–254.
- [38] P. A. Clapp, D. F. Evans, T. S. S. Sheriff, *Anal. Chim. Acta* **1989**, *218*, 331–334.

Received: April 25, 2011

Revised: July 6, 2011

Published online on November 15, 2011